2014 IEEE International Conference on Robotics & Automation (ICRA)
Hong Kong Convention and Exhibition Center
May 31 - June 7, 2014. Hong Kong, China

An Inertial-Based Human Motion Tracking System with Twists and Exponential Maps

Xi Chen, Jie Zhang, William R. Hamel, Jindong Tan

***Abstract*— Wearable inertial tracking is well accepted due to its convenience for free-style motion tracking with high accuracy. Traditionally, complicated high-order calculations for human kinematic modeling and inaccurate estimation of sensor placement are interfering the efficiency of real-time tracking. In order to tackle the challenges, a wearable human motion tracking system is developed by applying twists and exponential maps techniques. When the body segments are articulated by product of exponential maps, joint positions are continuously updated based on these techniques and their rotational angles are represented individually within the global frame. It is more efficient to achieve real-time motion tracking with low-order calculations. Meanwhile by applying the well-designed calibration procedure, it is more convenient to estimate a sensor's position and orientation regardless of knowing its placement. This paper presents our approach and exemplifies the assessment of proposed motion tracking system by several tests of limb and full body motion tracking. The comparisons with *Vicon* and *OptiTrack* motion capture systems verify satisfactorily high accuracy.**

I. INTRODUCTION

Real-time human motion tracking has been applied to numbers of biomedical areas, such as clinical gait analysis, exercise rehabilitation, fall detection, joint analysis and etc [1]–[4]. Several tracking technologies, such as mechanical tracking ($Gypsy\ 7^{TM}$), magnetic tracking ($Liberty^{TM}$) and visual tracking (*Vicon*, *Qualisys*, *OptiTrack*) have been in used for years. However, complex and vulnerable infrastructures of these tracking technologies limit their usage in the controlled volume, which makes it unpractical in the free-living environment .

Inertial tracking (*Xsens*) performs more natural to track human motions. As the development of sensor technology, wireless inertial tracking system is well accepted because of its small size, convenient installation, wireless communication, low power consumption and accurate monitoring of daily activities. The wearable Inertial Measurement Unit (IMU), which consists of accelerometers, gyroscopes and magnetometers, is less cumbersome to the subject. It allows for unlimited estimation of limb orientations under fast motions, which improves the performance of motion capture at anytime and anywhere. This research aims to develop a human body motion tracking system, which is capable of tracking arbitrary 3D motions, measuring joint angles and reconstructing a human model by taking advantages of wireless sensors.

In current research, a common procedure is firstly building a human kinematic model to simulate the functionality of human links and then coupling measured inertial data with the model to reconstruct 3D motions. Traditional inertial tracking algorithm mostly applies rotation matrix for representing rotations along each axis of joints. The inverse kinematics technique [5] is a major way to address body link connections, which uses product of rotation matrix to demonstrate the rotations of a joint with multiple DoFs and connect body segments through joints. As an obvious drawback, the number of parameters needed in rotation matrixes can be raised linearly when more body links are connected. The high-order calculations apparently increase the computational time for kinematic modeling and impact the feasibility of tracking in real time.

An approach to solve the challenge by adopting twists and exponential maps techniques is introduced in this paper. A small amount of parameters (low-order) enable rapid calculations of joint angles, so that kinematic modeling can satisfy the needs for real-time model reconstruction. Besides, fewer parameters than rotation matrix would be added to the system when connecting more body segments, which almost does not affect real-time motion tracking. Without large amount of calculations, wearable body motion tracking system can estimate joint position rapidly and suffice real-time tracking.

Human soft tissue artifact is a main source of errors, no matter the wearable sensors are mounted on a garment or directly attached to skin. Besides, the spatial relationship of segment axes in a joint is actually much more complicated than it appears according to human anatomical structure [6]. Both issues bring challenges to the chosen of IMU placement on human body in typical tracking methods. Kalman filter [5], [7] and Gauss-Newton method [8] are usually used to integrate multiple sensor measurements to increase the reliability of sensor placement. The challenging task would still be, basically, to accurately estimate the sensor placement. In the proposed system, a well-designed calibration procedure is developed to minimize the interference from IMU placement. Regardless of arbitrary IMU placement, the procedure can estimate its position and orientation and couple its placement with corresponding joint, so that following tracking can be operated based on the inertial data of corresponding joint but with less concern to the placement issue.

It will be useful to develop a wearable human body motion tracking system, which is convenient to be applied to free-

X. Chen, W. R. Hamel and J. Tan are with the Department of Mechanical, Aerospace and Biomedical Engineering, The University of Tennessee, Knoxville, TN, 37996, USA. J. Zhang is with the Beijing University of Chemical Technology, Beijing, China.

This work is partially supported by NSF grant 1309921. Jie Zhang is also supported by an International Science and Technology Cooperation Program of China (2011DFG13000).

style activities as well. The challenges of sensor placement and modeling rapidness, as a matter of fact, conceal the advantages of wearable tracking for use throughout our life. Even though traditional tracking technique achieves good accuracy, the relatively complex initial configuration would confuse subjects and sway them to attempt a long term testing. Developing a "mount-n-use" system, which is non-intrusive to our daily life, becomes the purpose of this research.

In this paper, a wearable body motion tracking system is introduced, which can estimate joint angles and demonstrate arbitrary 3D motions in real time. A quaternion-based orientation filter is employed to pre-process inertial measurements and eliminate noises. A well designed calibration procedure optimally estimates position and orientation of IMUs, regardless of arbitrary placement. Compared with traditional approach that uses rotation matrix based high-order calculations, proposed technique with low-order calculations appears more convenient in 3D motions reconstruction in real time. The twists and exponential maps techniques explicitly describe rigid body motions and articulate kinematic chains to achieve human modeling. The assessment of developed system is exemplified by comparisons with commercialized motion capture systems on estimating joint angles.

II. PROBLEM FORMULATION

A human body is modeled as an articulated model, which consists of 15 rigid body segments, 14 joints and 38 Degrees of Freedom (DoFs). It includes torso, head, upper limbs and lower limbs, as Figure 1 shows.

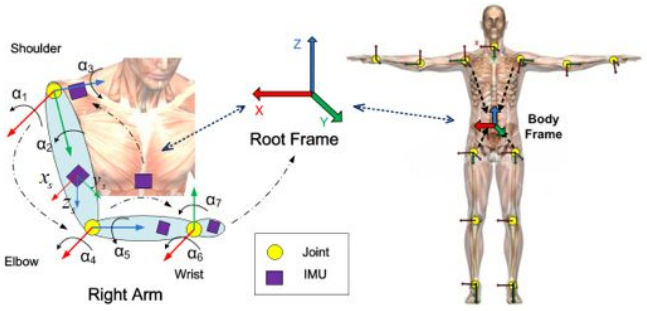

Fig. 1. Human full body model with joint coordinates and kinematic modeling of right arm with IMUs

Upper limb includes upper arm, forearm and hand, which has 10 DoFs in total. Shoulder is described as a ball and socket joint with 6 DoFs: 3-DoF rotations and 3-DoF translations. Rotation angles are assigned to flexion-extension α_1, internal-external α_2 and abduction-adduction α_3 rotations. Elbow is modeled as two hinge joints with non-intersecting axes [6]. It is described by 2 DoFs: flexion-extension α_4 and pronation-supination α_5 rotations. Wrist is modeled as an ellipsoid joint with 2 DoFs: flexion-extension α_6 and radial/ulnar deviation α_7 rotations. For the other side, similarly, the rotation angles $\alpha_8 \sim \alpha_{14}$ are assigned to axes of shoulder, elbow and wrist joint.

Torso provides the orientation of body and it includes two joints: neck has 3 DoFs and waist has 3 DoFs, so that the spinal movements can be simplified as the rotations around waist joint. Neck movement is excluded in this work and rotation angles $\alpha_{15} \sim \alpha_{17}$ are assigned to waist joint. Lower limbs have similar structure as upper limbs but perform less complicated motions. Hip joint has 3 DoFs rotations: flexion-extension α_{18}, internal-external α_{19} and abduction-adduction α_{20}. Knee joint has only flexion-extension α_{21} rotation. Ankle joint has complicated anatomy [9], it is simplified as only flexion-extension α_{22} rotation. For the other side, rotation angles are from α_{23} to α_{27}.

An embedded quaternion-based orientation filter is utilized to pre-process and denoise raw IMU data and output filtered quaternion. In Figure 1, the rotation angles of shoulder joint α_1, α_2 and α_3, elbow joint α_4, α_5 and wrist joint α_6, α_7 are expressed by measurement quaternion ${}_S\mathbf{q}$, ${}_E\mathbf{q}$ and ${}_W\mathbf{q}$ for shoulder frame, elbow frame and wrist frame. Three quaternions integrate the movements of three arm joints instead of seven rotational matrixes $R(\alpha_1)...R(\alpha_7)$ for simplification. During the movements, these three measurement values of quaternion compare with estimated quaternions ${}_S\tilde{\mathbf{q}}$, ${}_E\tilde{\mathbf{q}}$ and ${}_W\tilde{\mathbf{q}}$ for shoulder frame, elbow frame and wrist frame, and approach them after each time span t to minimize the difference $\delta = \|({}_S\mathbf{q}, {}_E\mathbf{q}, {}_W\mathbf{q}) - ({}_S\tilde{\mathbf{q}}, {}_E\tilde{\mathbf{q}}, {}_W\tilde{\mathbf{q}})\|_t$. Same idea is applied to other joints of the human body to update and keep the joint motions being tracked.

After estimating rotation angles of each joint, we are aiming at estimate real-time update of joint position. As a principal part, real-time position of IMUs within the Root Frame are calculated by proposed tracking technique first. Since the relative position between individual IMU and corresponding joint is changeless, joints position in the Root Frame can be derived by translations from IMUs' position.

III. MOTION TRACKING WITH TWIST AND EXPONENTIAL MAPS

In this section, a body tracking system with twists and exponential maps techniques is introduced. Due to the superiority of quaternion-based rotation representation over Euler angles and rotation matrix, filtered unit quaternions by embedded orientation filter of IMUs are used as system input for calculating the twist motions. Exponential map for twists simplifies the representation of rotation by reducing the computing complexity to one matrix per joint, compared with one matrix per DoF in the traditional method. In order to track motions of a body with multiple joints and segments, the product of exponential maps, which borrows the idea from the *forward kinematics* technique, is employed to express the kinematic chain. The motion reconstruction will be accomplished based on human kinematic chains and rotation angles of each joint.

A. Quaternion-based Orientation Filter

In our previous work [10], an adaptive-gain complementary filter was developed and combined with Gauss-Newton optimization algorithm to determine the orientation

of the gyroscope measurement error. The filter consumes short computing time, which satisfies the needs for real-time orientation measurement, and filtered quaternion of the Root Frame ${}_{\mathbb{R}}\mathbf{q}$ denotes the IMU output within $\mathbb{R}$.

B. Twists and Exponential Maps

The representation of general body motions includes both rotations and translations. Here we have two coordinate frames $\mathbb{A}$ and $\mathbb{B}$: let $p_{\mathbb{AB}} \in \mathbb{R}^3$ be the position vector from the origin of frame $\mathbb{A}$ to the origin of frame $\mathbb{B}$, and $R_{\mathbb{AB}} \in SO(3)$ (special Orthogonal group) be the orientation of frame B, relative to frame $\mathbb{A}$. A configuration of the system consists of the pair $(p_{\mathbb{AB}}, R_{\mathbb{AB}})$, and the configuration space of the system is the product space of $\mathbb{R}^3$ with $SO(3)$, which is denoted as $SE(3)$

$$\begin{aligned} SE(3) &= \{(p_{\mathbb{AB}}, R_{\mathbb{AB}}) : p_{\mathbb{AB}} \in \mathbb{R}^3, R_{\mathbb{AB}} \in SO(3)\} \\ &= \mathbb{R}^3 \times SO(3) \\ SO(3) &= \{R_{\mathbb{AB}} \in \mathbb{R}^{3\times3} : R_{\mathbb{AB}} R_{\mathbb{AB}}^T = I, \det R_{\mathbb{AB}} = +1\} \end{aligned}$$

More concretely, let $q_{\mathbb{S}}$, $q_{\mathbb{E}} \in \mathbb{R}^3$ be the coordinates of a point q relative to local Shoulder Frame $\mathbb{S}$ and local Elbow Frame $\mathbb{E}$ respectively. Let $R_{\mathbb{SE}}$ indicates 3 DoF rotations of point q needed from $\mathbb{S}$ to $\mathbb{E}$, through rotations α_1, α_2 and α_3. Given $q_{\mathbb{S}}$, $q_{\mathbb{E}} = p_{\mathbb{SE}} + R_{\mathbb{SE}} \cdot q_{\mathbb{S}}$ shows the transformation. Let $g_{\mathbb{SE}} = (p_{\mathbb{SE}}, R_{\mathbb{SE}}) \in SE(3)$ be the specification of the configuration of the frame $\mathbb{E}$ relative to the frame $\mathbb{S}$. Using *homogeneous representation*, the linear form transformation is represented as

$$\bar{q}_{\mathbb{E}} = \begin{bmatrix} q_{\mathbb{E}} \\ 1 \end{bmatrix} = \begin{bmatrix} R_{\mathbb{SE}} & p_{\mathbb{SE}} \\ \mathbf{0} & 1 \end{bmatrix} \begin{bmatrix} q_{\mathbb{S}} \\ 1 \end{bmatrix} = \bar{g}_{\mathbb{SE}} \bar{q}_{\mathbb{S}} \tag{1}$$

Euler angles are commonly used to constrain a rotation matrix R to $SO(3)$, but they suffer from singularities and don't lead to a simple formulation. In contrast, the twist representation provides a more elegant solution and leads to a very simple linear representation of the motion model. For each homogeneous matrix $\bar{g} \in SE(3)$, there is a corresponding twist in the tangent space $se(3)$, we define

$$\begin{aligned} se(3) &= \{(v, \hat{\omega}) : v \in \mathbb{R}^3, \hat{\omega} \in so(3)\} \\ so(3) &= \{S \in \mathbb{R}^{3\times3} : S^T = -S\} \end{aligned}$$

where $\hat{\omega} \in so(3)$ here is the skew-symmetric matrix of the unit axis ω of a rotation. v is the velocity of a point attached to the joint.

In homogeneous coordinates, we define $\xi \in \mathbb{R}^6$ represents the twist coordinates and a twist $\hat{\xi} \in se(3)$ as

$$\hat{\xi} = \begin{bmatrix} v \\ \omega \end{bmatrix}^{\wedge} = \begin{bmatrix} \hat{\omega} & v \\ \mathbf{0} & 0 \end{bmatrix} \in \mathbb{R}^{4\times4} \tag{2}$$

where $v = -\omega \times r$ and r denotes the origin of rotation axis in the twist $\hat{\xi} \in se(3)$. The exponential of $\theta\hat{\omega}$, $e^{\theta\hat{\omega}}$, is an element of $SE(3)$ and it indicates the rotations during the movements, where θ is the angle of rotation about ω. It can be calculated by the *Rodrigues' formula*: $e^{\theta\hat{\omega}} = I + \hat{\omega}sin\theta + \hat{\omega}^2(1 - cos\theta)$. Elements from $se(3)$ are mapped to $SE(3)$ by using the exponential map for twists as shown in following equation

$$\begin{aligned} e^{\theta\hat{\xi}} = \begin{bmatrix} e^{\theta\hat{\omega}} & (I - e^{\theta\hat{\omega}})(\hat{\omega}v + \omega\omega^T v\theta) \\ \mathbf{0} & 1 \end{bmatrix} \quad \omega \neq \mathbf{0} \\ e^{\theta\hat{\xi}} = \begin{bmatrix} I & v\theta \\ \mathbf{0} & 1 \end{bmatrix} \quad \omega = \mathbf{0} \end{aligned} \tag{3}$$

The 3-DoF rotation of shoulder relative to the Elbow Frame can be represented by $(e^{\theta\hat{\omega}})_{\mathbb{SE}}$ and the transformation from $\mathbb{S}$ to $\mathbb{E}$, which includes rotations and translations, is shown by a 4×4 matrix $(e^{\theta\hat{\xi}})_{\mathbb{SE}}$, instead of the multiplication of three 3×3 rotational matrixes $R(\alpha_1) \cdot R(\alpha_2) \cdot R(\alpha_3)$. One body link transformation relationship is introduced above and the example of a connection of upper body links will be discussed next.

Firstly, IMUs are calibrated in $\mathbb{R}$. Their initial orientation ${}_{\mathbb{R}}\mathbf{q}_I$ translate to θ_I for later use. Here uses I to denote initial state. After attaching IMUs to the human body, orientation measurements on the body are rotated from initial ${}_{\mathbb{R}}q_I$ to ${}_{IB}\mathbf{q}$ for the IMU corresponding to waist in Body Frame Σ_{body}, ${}_{IS}\mathbf{q}$, ${}_{IE}\mathbf{q}$ and ${}_{IW}\mathbf{q}$ for the IMU corresponding to shoulder, elbow and wrist. In this procedure, the subject is asked to stand in order to mount the IMUs. The local coordinate of waist, shoulder, elbow and wrist refer to $\mathbb{R}$ are initially defined as ${}^{\mathbb{R}}_{B}\mathbf{q}_{initial}(= \mathbb{R})$, ${}^{\mathbb{R}}_{S}\mathbf{q}_{initial}$, ${}^{\mathbb{R}}_{E}\mathbf{q}_{initial}$ and ${}^{\mathbb{R}}_{W}\mathbf{q}_{initial}$. The relationship between local joints coordinate and corresponding IMUs are shown as

$$\begin{aligned} {}^{\mathbb{R}}_{B}\mathbf{q}_{initial} &= {}^{S}_{IB}\mathbf{q} \otimes {}_{IB}\mathbf{q} \\ {}^{\mathbb{R}}_{S}\mathbf{q}_{initial} &= {}^{S}_{IS}\mathbf{q} \otimes {}_{IS}\mathbf{q} \\ {}^{\mathbb{R}}_{E}\mathbf{q}_{initial} &= {}^{E}_{IE}\mathbf{q} \otimes {}_{IE}\mathbf{q} \\ {}^{\mathbb{R}}_{W}\mathbf{q}_{initial} &= {}^{W}_{IW}\mathbf{q} \otimes {}_{IW}\mathbf{q} \end{aligned} \tag{4}$$

where the relationship quaternion ${}^{S}_{IB}\mathbf{q}$, ${}^{S}_{IS}\mathbf{q}$, ${}^{S}_{IE}\mathbf{q}$ and ${}^{S}_{IW}\mathbf{q}$ will be used for updating real-time rotation measurements of joint quaternions.

We assume the starting position of the initial configuration of the Body Frame is known as ${}^{\mathbb{R}}P_B$. An IMU mounted on the chest is used to estimate the orientation of upper trunk and two IMUs mounted on each scapula (sc-IMU) are measuring the linear acceleration of shoulder movements. The translational calculation from body to shoulder $p_{\mathbb{BS}}$ initially includes ${}^{\mathbb{R}}P_B$, initial spacial relationship of shoulder relative to waist ${}_{I}p_{\mathbb{BS}}$ and the real-time update of the shoulder position from sc-IMU inertial measurements p_{sc-IMU} within Σ_{body}

$$p_{\mathbb{BS}} = {}^{\mathbb{R}}P_B + {}_{I}p_{\mathbb{BS}} + p_{sc-IMU} \tag{5}$$

Following the idea of forward kinematics, the aim here is to estimate the updated shoulder position within $\mathbb{R}$. As the subject moves, the quaternion of the chest IMU continuously updates waist joint quaternion measurement ${}^{\mathbb{R}}_{B}\mathbf{q} = {}^{S}_{IB}\mathbf{q} \otimes {}_{IB}\mathbf{q}$. With the waist quaternion measurements are calculated, the shoulder joint position can be updated by

$${}^{\mathbb{R}}_{B}\mathbf{q} \rightarrow \theta_B, \omega_B \qquad \{\theta_B, \omega_B, p_{\mathbb{BS}}\} \overset{exp\ map}{\Longrightarrow} {}^{\mathbb{R}}P_S \tag{6}$$

where ${}^{\mathbb{R}}P_S$ denotes updated shoulder position within $\mathbb{R}$.

The translational calculation from shoulder to elbow $p_{\mathbb{SE}}$ is achieved by combining ${}^{\mathbb{R}}P_S$ and initial spacial relationship of elbow relative to shoulder ${}_{I}p_{\mathbb{SE}}$ within $\Sigma_{shoulder}$. As the subject moves, the quaternion of s-IMU (denotes the IMU corresponding to shoulder) continuously updates shoulder joint quaternion ${}^{\mathbb{R}}_{S}\mathbf{q} = {}^{S}_{IS}\mathbf{q} \otimes {}_{IS}\mathbf{q}$. With shoulder quaternion are calculated, the elbow joint position can be updated by

$$ {}^{\mathbb{R}}_{S}\mathbf{q} \rightarrow \theta_S, \omega_S \qquad \{\theta_S, \omega_S, p_{\mathbb{SE}}\} \overset{exp\ map}{\Longrightarrow} {}^{\mathbb{R}}P_E \tag{7} $$

where ${}^{\mathbb{R}}P_E$ denotes updated elbow position within $\mathbb{R}$. By applying the same rules, the updated position of wrist and hand can be achieved and denoted by ${}^{\mathbb{R}}P_W$ and ${}^{\mathbb{R}}P_{hand}$.

The rotations of each joint of above example are represented by $\{\theta_B, \theta_S, \theta_E, \theta_W\}$ with corresponding twists $\{\hat{\xi}_B, \hat{\xi}_S, \hat{\xi}_E, \hat{\xi}_W\}$. The exponential map for twists of each joint is in the form of $e^{\theta\hat{\xi}}$, as Equation (3) shows. If the initial configuration of one IMU corresponding to $\mathbb{R}$ is $g(0)$, the final configuration of the IMU corresponding to $\mathbb{R}$ with rotation angle θ is given by $g(\theta) = e^{\theta\hat{\xi}}g(0)$.

Above arm connection is demonstrated by the product of all joints' exponential maps $\prod_{i=B}^{W} e^{\theta_i\hat{\xi}_i} = e^{\theta_B\hat{\xi}_B} \cdot e^{\theta_S\hat{\xi}_S} \cdot e^{\theta_E\hat{\xi}_E} \cdot e^{\theta_W\hat{\xi}_W}$. If we let $g_{wrist,hand}(0)$ represent the initial configuration of hand *w.r.t* wrist, the final configuration of hand *w.r.t* the Body Frame $g_{body,hand}$, connected by rotation angles $\Theta = (\theta_B, \theta_S, \theta_E, \theta_W)$ is given by

$$ \begin{aligned} g_{body,hand}(\Theta) &= \prod_{i=B}^{W} e^{\theta_i\hat{\xi}_i} \cdot g_{wrist,hand}(0) \\ &= exp(\sum_{i=B}^{W} \theta_i\hat{\xi}_i) \cdot g_{wrist,hand}(0) \end{aligned} \tag{8} $$

The advantage of twists and exponential maps techniques are revealed by transforming the multiplication of exponentials to summations of exponentials, which substantially reduces the complexity of motion estimation of multiple body links, compared with rotation matrix representations.

C. Kinematic Chains and Full Body Motion

A human body model consists of a set of body segments connected by joints. For upper limbs and lower limbs, four kinematic chains are modeled and branch out the torso. The goal of constructing human kinematic chain is to find the independent configuration for each joint and their relationship within the Root Frame, such as Figure 2 shows.

Four kinematic chains of upper and lower limbs are built to describe 10-DoF arm movements and 5-DoF leg movements. For the upper limb, a kinematic chain that expressing the wrist frame relative to the body frame is modeled as

$$ \begin{aligned} g_{body,hand}(\Theta) = exp(\theta_{body}\hat{\xi}_{body} + \theta_{shoulder}\hat{\xi}_{shoulder} + \theta_{elbow}\hat{\xi}_{elbow} \\ + \theta_{wrist}\hat{\xi}_{wrist}) \cdot g_{wrist,hand}(0) \end{aligned} \tag{9} $$

and for the lower limb, the ankle frame relative to the body frame is modeled as

$$ \begin{aligned} g_{body,foot}(\Theta) = exp(\theta_{body}\hat{\xi}_{body} + \theta_{hip}\hat{\xi}_{hip} + \theta_{knee}\hat{\xi}_{knee} \\ + \theta_{ankle}\hat{\xi}_{ankle}) \cdot g_{ankle,foot}(0) \end{aligned} \tag{10} $$

where Θ represents the set of rotation angles of joints involved in the final configuration.

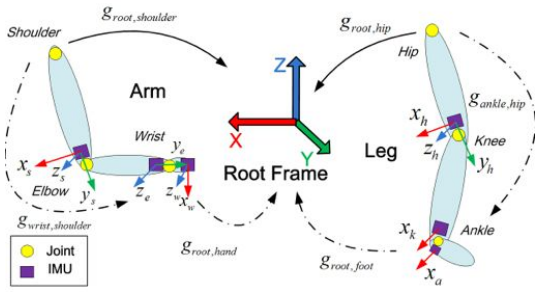

Fig. 2. Kinematic chains of upper and lower extremities.

A full body model is reconstructed by linking all the limb kinematic chains to the torso and mapping individual sensor frames into $\mathbb{R}$. Full body motion estimation represents the twist of all the body segments under the Root Frame, so that the human motion can be displayed as a coherent reconstruction. The IMU on the chest is used to capture the motion of waist joint and represent torso direction. Based on the fact that all the limb chains are connected to torso, the Root Frame is placed at human waist. For example, the motion of a lower arm relative to human foot is shown by

$$ \begin{aligned} g_{ankle,elbow}(\Theta) = exp(\sum_{ankle}^{hip} \theta_i\hat{\xi}_i + \sum_{hip}^{body} \theta_i\hat{\xi}_i + \sum_{body}^{shoulder} \theta_i\hat{\xi}_i + \\ \sum_{shoulder}^{elbow} \theta_i\hat{\xi}_i) \cdot g_{shoulder,elbow}(0) \end{aligned} \tag{11} $$

IV. EXPERIMENTS

A. Experimental Setup

The IMU was developed in our lab and the detail was introduced in [11]. The commercialized *Vicon* and *OptiTrack* motion capture systems are separately utilized as the benchmark. Six cameras are set up at the frequency of $100Hz$, while IMUs are working at $40Hz$. A series of upper limb and full body motions are designed to validate our tracking system. Three ranges of movements are executed for both the upper limb tracking and full body tracking. Each range is repeated twice to clearly demonstrate the motion and apart from other ranges. Two participants are asked to test developed system by using these motions. Before the tests, the participants are required to stand upright in T-pose to attach IMUs on the body. During the tests, motion capture system and our tracking system are manually started to capture the motions simultaneously. The inertial measurements from IMUs are analyzed and joint positions captured by *Vicon* and *OptiTrack* are recorded for later calculations and comparisons.

B. Upper Limb Motion Tracking

Figure 3 shows a screenshot of the motion tracking procedure. The participant with reflective markers affixed on the arm is asked to move gently as designed motions and *Vicon*

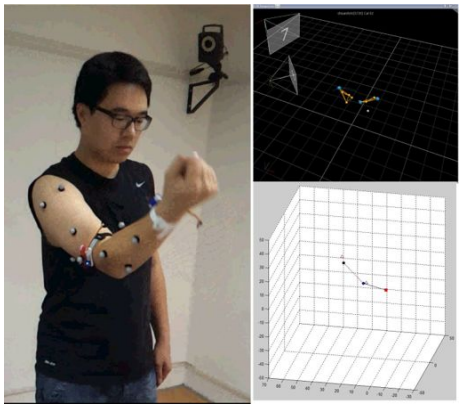

Fig. 3. Upper limb tracking procedure

system captured his motion simultaneously and animated, as shown in the top right of Figure 3. Inertial measurements are transmitted wirelessly to the computer and tracked motions are reconstructed as shown in the bottom right of Figure 3. Each test procedure is analyzed graphically as curves of angle against frame. After the motion data are transmitted to the computer, angles between two adjacent body segments are estimated. By comparing with the benchmark results from *Vicon*, the accuracy of developed motion tracking system can be evaluated.

In the tests, shoulder angles and elbow angles are calculated from IMU data for comparison with *Vicon* truth. In the figures, the red curve represents angles calculated from *Vicon* system and the blue curve shows the angles estimated by proposed tracking system based on IMU measurements.

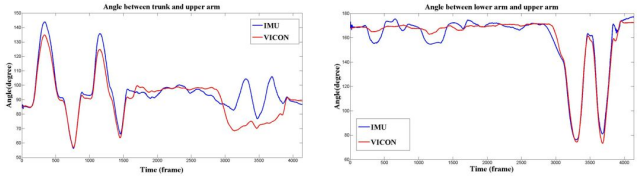

(a) angles between upper arm and trunk (b) angles between upper and lower arm

Fig. 4. Angle comparison results.

Figure 4(a) shows the angle between body trunk and upper arm. The 1^{st} range movement, arm lifting up-falling back, is shown by the first two wave peaks and troughs. The 2^{nd} range movement, arm swinging to left-right, is represented by the following flat curve. For these two ranges, the IMU tracking performs well in matching the *Vicon* truth. However for the 3^{rd} range, lower arm flexion-extension, IMU tracking does not match *Vicon* data very well. The reason of this unmatch is from additional vibration of the soft tissue artifact, due to contractions of biceps brachii. Even though the IMU is placed on the flat sulcus bicipitalis lateralis, it can hardly avoid vibrations but try to minimize it. This little but inevitable vibration is magnified by sensitive IMU sensors and then lost precise capture. The average difference for these two angle curve is 6.3°, and the similarity (correlation) of two curves is 0.8354.

Figure 4(b) shows the angle between lower arm and upper arm. During the 1^{st} and 2^{nd} range movements, this angle should not vary too much because of fixed angle of elbow joint. It can be observed from the curves, IMU tracking in the 1^{st} and 2^{nd} range fluctuates. The fluctuation at first is from gyroscope errors, since the gyroscope encountered a sudden start of movement. Although embedded orientation filter (in Section III-A) in the IMU is capable of calibrating and recovering the impact from errors, a short time is needed. Whereafter, proposed filter takes effect gradually on the 2^{nd} range movement and corrects the orientation of IMU tracking, which causes the curve remaining flat. The 3^{rd} range performs elbow flexion-extension and the IMU tracking matches the *Vicon* truth mostly and is not affected by previous fluctuation clearly. The average difference for these two angle curve is 3.5° and the similarity (correlation) of two curves is 0.9824.

C. Full Body Motion Tracking

A 3-range movement is performed in the full body tracking procedure. The participant with markers and IMUs is started with "T-pose" and is requested to accomplish arm abduction, arm forward flexion, standing leg lifts and keeping balance, as are shown in Figure 5(b). Figure 5(a) describes the placement of IMUs and markers on the body. For full body tracking, *OptiTrack* motion capture system is used as the benchmark. Similar as the upper limb tracking test, full body tracking is analyzed as curves of angle against frame. Four angles are our concern and calculated for comparison: elbow angles (between upper arm and lower arm) for each arm and knee angles (between thigh and shank) for each leg. Compared with the angles calculated from *OptiTrack* truth, the accuracy for developed system is further evaluated.

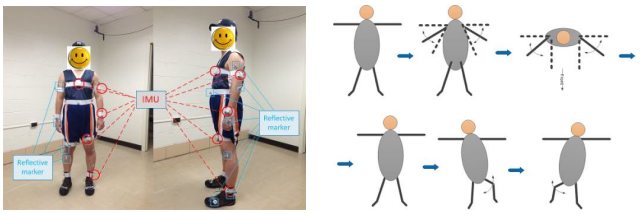

(a) (b)

Fig. 5. IMU and reflective marker placement and planned motions

In the following comparisons, the red curve represents angles calculated from *OptiTrack* camera system and the blue one shows angles estimated by our developed system.

Figure 6(a) and Figure 6(b) shows the angle between upper arm and lower arm for left arm and right arm, which are elbow flexion-extension angles. Three ranges of movements are performed during the test. First two ranges of movements are basically arm motions. Because the elbow is not fixed when rotating shoulder joint, the figure clearly shows angle changes of elbow joint by four wave troughs and fluctuations. The 3^{rd} range of movements is lifting legs while keeping body balance. During these movements, arms shake a bit for

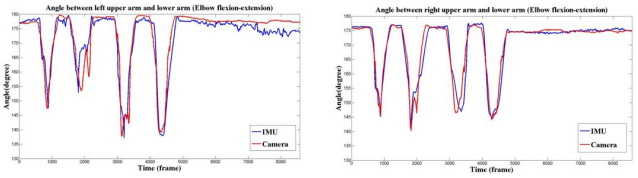

(a) Angle changes of left elbow flexion-extension

(b) Angle changes of right elbow flexion-extension

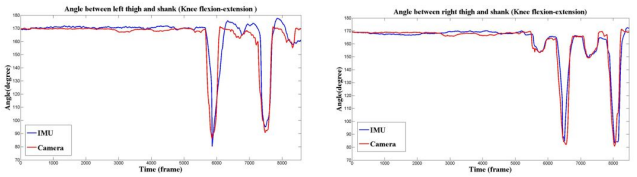

(c) Angle changes of left knee flexion-extension

(d) Angle changes of right knee flexion-extension

Fig. 6. Angle changes during elbow and knee flexion-extension movements for both sides

keeping the balance, which is reflected as the fluctuations of the IMU curve in the 3^{rd} range. The overall results show that angles from IMU and from camera system match very well. The fluctuations of the IMU curve are basically caused by sensitive sensing, while the camera software processes the marker position to make it smoother. The sample rate for the camera system is $100Hz$ and for IMU is $40Hz$, thus the interpolation procedure is applied to inertial data for comparison.

Figure 6(c) and Figure 6(d) shows the angle between thigh and shank for left leg and right leg, which are knee flexion-extension angle. The 3^{rd} range of movement is lifting thigh and bending knee, so the two wave troughs denote these movements. From the figure, it is clear that IMU curves match the camera truth better for right leg than left leg. This result can be explained that while lifting right leg, left leg is able to better keep body balance than the other side, since our subject is right-handed. Because of the same reason, the right arm has less fluctuations during the 3^{rd} range of movements. Although at the end of the test, the angle difference increases, the orientation filter in the IMU will be able to calibrate and recover the inertial data quickly when subject's motion turns into gentle and slow. For overall results, our inertial tracking technique is capable of capturing and calculating the body motions accurately. The average difference of angle comparisons for these four figures and their similarity (correlation) are summarized in Table I. For

TABLE I

COMPARISON OF IMU ANGLE AND CAMERA ANGLE FOR EACH FIGURE

	Left	Right	Average Difference	Correlation
Elbow	×		2.6°	0.9349
		×	1.5°	0.9625
Knee	×		4.2°	0.9052
		×	3.1°	0.9447

a right-handed subject, a preliminary find is for keeping the body balance, the right arm and left leg are more capable than the other side, with less shakes and fluctuations. More angles of human joints also can be calculated by using developed tracking system, and by analyzing joints rotations and monitoring the reconstructed human motions, the status of a subject is achievable remotely and in either virtual display or quantitative summary in real-time process.

V. CONCLUSIONS

In this paper, a wearable motion tracking system is developed. IMUs are mounted on body segments and regardless of their placement, a well-designed calibration procedure can estimate the position and orientation accurately. Inertial measurements are pre-processed by developed quaternion-based orientation filter for eliminating noises. The twists and exponential maps techniques describe body movements accurately and articulate body segments to build a human model. Our low-order computational system enables the needs for real-time motion reconstruction and modeling. Besides, quantitative status of tracked subject can be analyzed and diagnosed rapidly. The comparisons with commercialized *Vicon* and *OptiTrack* motion capture systems assess the accuracy of proposed body motion tracking system. Analysis of joint angle provides quantified tracking results and accurate illumination for motion status.

REFERENCES

[1] B. Rosenhahn and T. Brox, "Scaled motion dynamics for markerless motion capture," in *IEEE Conference on Computer Vision and Pattern Recognition*, pp. 1–8, June 2007.

[2] H. Liu and R. Chellappa, "Markerless monocular tracking of articulated human motion," in *IEEE International Conference on Acoustics, Speech and Signal Processing*, vol. 1, pp. 693–696, April 2007.

[3] G. Pons-Moll, A. Baak, T. Helten, M. Müller, H.-P. Seidel, and B. Rosenhahn, "Multisensor-fusion for 3d full-body human motion capture," in *Computer Vision and Pattern Recognition (CVPR), 2010 IEEE Conference on*, pp. 663 –670, 2010.

[4] H. He, S. S. Ge, and Z. Zhang, "A saliency-driven robotic head with bio-inspired saccadic behaviors for social robotics," *Autonomous Robots*, vol. 36, no. 3, pp. 225–240, 2014.

[5] R. Zhu and Z. Zhou, "A real-time articulated human motion tracking using tri-axis inertial/magnetic sensors package," *IEEE Transactions on Neural Systems and Rehabilitation Engineering*, vol. 12, pp. 295–302, June 2004.

[6] A. Cutti, A. Giovanardi, L. Rocchi, A. Davalli, and R. Sacchetti, "Ambulatory measurement of shoulder and elbow kinematics through inertial and magnetic sensors," *Medical and Biological Engineering and Computing*, vol. 46, pp. 169–178, 2008. 10.1007/s11517-007-0296-5.

[7] J. Lin and D. Kulić, "Human pose recovery using wireless inertial measurement units.," *Physiol Meas*, vol. 33, no. 12, pp. 2099–2115, 2012.

[8] Y. Lee and W. Chung, "Wireless sensor network based wearable smart shirt for ubiquitous health and activity monitoring," *Sensors and Actuators B: Chemical*, vol. 140, no. 2, pp. 390–395, 2009.

[9] A. Lundberg, O. Svensson, G. Nemeth, and G. Selvik, "The axis of rotation of the ankle joint," *Journal of Bone & Joint Surgery, British Volume*, vol. 71-B, no. 1, pp. 94–99, 1989.

[10] Y. Tian, H. Wei, and J. Tan, "An adaptive-gain complementary filter for real-time human motion tracking with marg sensors in free-living environments," *IEEE Transactions on Neural Systems and Rehabilitation Engineering*, no. 99, p. 1, 2012.

[11] X. Chen, S. Hu, Z. Shao, and J. Tan, "Pedestrian positioning with physical activity classification for indoors," in *IEEE International Conference on Robotics and Automation*, pp. 1311–1316, May 2011.